Presented at the 32nd European PV Solar Energy Conference and Exhibition, 20-24 June 2016, Munich, Germany

INVESTIGATION OF THERMOMECHANICAL STRESS IN SOLAR CELLS WITH MULTI BUSBAR INTERCONNECTION BY FINITE ELEMENT MODELING

Li Carlos Rendler[1], Achim Kraft[1], Christian Ebert[2], Steffen Wiese[3], and Ulrich Eitner[1]
[1]Fraunhofer Institute for Solar Energy Systems ISE, Heidenhofstraße 2, 79110 Freiburg, Germany
[2]SCHMID Group | Gebr. SCHMID GmbH, Robert-Bosch-Str. 32-36, 72250 Freudenstadt, Germany
[3]Saarland University, Microintegration and Reliability, Campus A5 1, 66123 Saarbruecken, Germany

ABSTRACT: The interconnection of silicon solar cells by soldering causes thermomechanical stress due to different coefficients of thermal expansion of the materials involved, especially copper and silicon. In contrast to the current standard interconnection technology, using three to five flat ribbons to be soldered on continuous or segmented busbars on the solar cells front side and on large contact pads on the solar cells rear side, the Multi Busbar concept uses twelve to fifteen round solder coated copper wires to be soldered on a large number of small contact pads for each polarity.
In this paper we present two finite element models, one for a solar cell with a common busbar-based interconnection and a second one for a solar cell using the Multi Busbar interconnection approach to analyze and compare the distribution of the thermomechanical stress induced by the cell interconnection. The results show only a slight vertical deformation of a contacted solar cell of 0.4 mm for the three busbar design and 2.2 mm for the Multi Busbar interconnection technology due to the non-symmetric pad layout and the aluminum metallization on the rear side. However, most parts of the copper interconnector (ribbons and wires) are plastically deformed because the tensile stress exceeds the yield strength of 100 MPa. In addition, the results indicate that there is only slight tensile stress in most parts of the silicon solar cell after the soldering process. For both interconnection technologies we detect local stress peaks and, on the rear side of the solar cells near the outermost contacts, we determine areas where the tensile stress reaches levels above 200 MPa that potentially cause defects.

Keywords: FEM, Modeling, Multi Busbar, PV Materials, Thermomechanical Stress, Wire Interconnection

1 INTRODUCTION

Standard silicon solar cells are interconnected by soldering three to five solder coated copper ribbons onto screen-printed contacts on both sides of the solar cell. The most common concept uses continuous or segmented screen printed busbars on the front side combined with around six large contact pads on the rear side. However, there are alternative concepts on the market that show several advantages. Two innovative examples are Schmid's Multi Busbar (MBB) concept, working with twelve to fifteen round wires, soldered on both sides on small contact pads of a solar cell by infrared light [1-5] as well as the Smart Wire Connection Technology of Meyer Burger, using around thirty wires on both sides that are embedded in a polymer foil and interconnected during the lamination process directly with the contact fingers [6]. Both concepts use round wires instead of flat ribbons as well as adapted metallization layouts on the solar cell surfaces. The round shape of the wire interconnectors promotes a redirection of incoming light on the solar cells front surface. Using contact pads instead of continuous busbars and lowering the finger thickness results in a significant reduction of the silver consumption. By using a higher number of interconnectors on the solar cells surfaces the concept shows particular high reliabilities because there is a redundancy in the current collection paths and the series resistance increases less in case of defects like cell cracks, failure of solder joints or even broken interconnectors. Additionally, a reduction of the series resistance caused by a more homogenous current collection has been shown [1-4].

All these concepts have in common, that after the solder process the silicon solar cell and the copper interconnectors are rigidly fixed by the solder. The different coefficients of thermal expansion (CTEs) cause thermomechanical stress in the interconnected cell. In the interconnection process, where the cell is heated up to temperatures above the solder melting point, as well as during its lifetime, a solar module undergoes several temperature changes that might cause defects resulting from thermomechanical stress [7]. In addition to the CTE, the mechanical properties of the interconnector, for example the Young's modulus and the yield strength, have a significant influence on the thermomechanical stress [8]. Defects of solder joints like cracks or delamination of layers result in an increase of a module's series resistance and therefore reduce the module efficiency.

The distribution of the thermomechanical stress caused by the interconnection process is determined by means of simulation models using the finite elements method (FEM). In previous work we investigated the relevant material data that serve as input parameters for FEM simulations. Additionally, by simulating the single-side soldering of a solar cell section and showing the good agreement of experimental and model results, we demonstrated that a FEM model based on the used parameters deliver reasonable results [7]. We use two FEM models to analyze the stress distribution in solder joints after the interconnection process of a common solar cell with three busbars (3BB) as well as in a solar cell with the wire based MBB interconnection. By analyzing the respective stress level caused by the solder process it is possible to analyze if an interconnection concept is prone to defects like cracks or delamination. Additionally, we determine where such defects most likely occur, which is crucial for further development of the interconnection technology.

2 MODELING

The model geometry for both analyzed inter-connection approaches (3BB and MBB) consists of a section of a silicon solar cell (156 x 10.2 x 0.175 mm³).

To reduce computational memory consumption and calculation time, only one fourth of the whole cell section is taken into account and two symmetry conditions, longitudinal and transversal, are applied to the cut planes as shown in figure 1 and 3. Both model geometries include screen-printed silver-based contact areas on both sides. Contact and redundancy fingers are not modeled since their influence on thermomechanical stress is expected to be negligible. On the rear side, we simulate a screen-printed aluminum-based metallization layer with a thickness of 8 µm (3BB) or respectively 30 µm (MBB) that includes square shaped cut-outs in the area of the contact pads as shown in figure 2 and 4.

2.1 Three busbar geometry

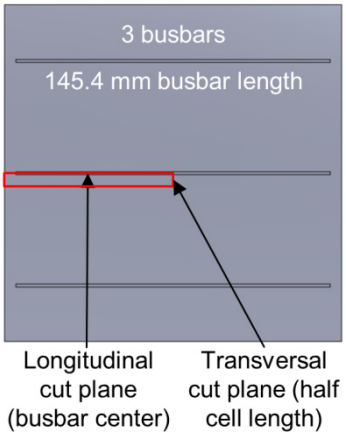

Figure 1: Schematic drawing of the front surface of a common silicon solar cell with three continuous busbars on the cell front side. The red box indicates the area used in the FEM model. Additionally, cut planes to apply symmetry conditions that reduce the model complexity are shown.

The 3BB cell section includes one quarter of a busbar (0.675 x 72.7 x 0.014 mm³) on the front side as well as half of three large contact pads (9.0 x 1.6 x 0.008 mm³) on the rear side as pictured in figure 2.

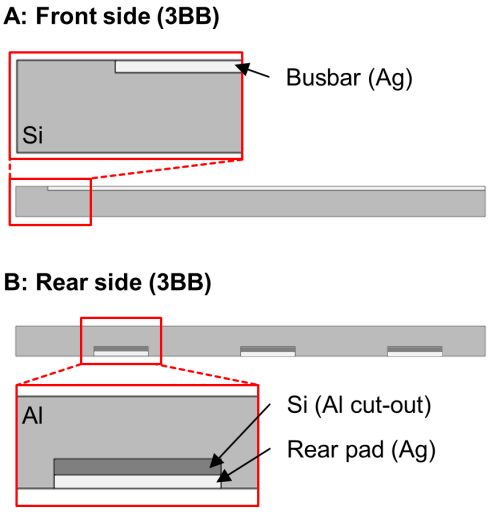

Figure 2: Metallization layout on the front (A) and the rear side (B) of the 3BB model geometry.

2.1 Multi Busbar geometry

In the MBB model we simulate a metallization geometry including 16 contact pads on the front and 20 pads on the rear side of the cell section. The physical dimensions for the MBB model are determined by numerous microsections and confocal microscope imaging shown in previous work [7].

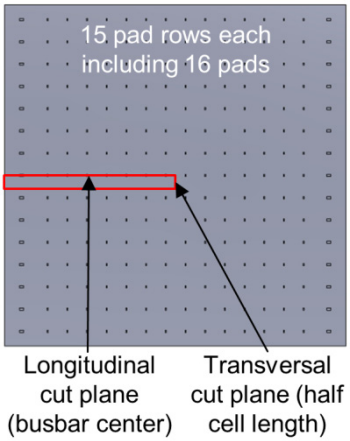

Figure 3: Schematic drawing on the front surface of a MBB solar cell with 15 pad rows, each including 16 pads. The red box shows the area that is used as geometry in the FEM model.

On the front side, the outermost pads have a size of 2 x 1 mm². The inner pads measure 0.45 x 1 mm² in size. On the rear side of the model geometry, which is displayed in figure 4, there are cut-outs in the aluminum layer and the pads of each pad group with a size of 2 x 1.6 mm² (outer pads) or respectively 0.5 x 1.6 mm² (inner pads). The height of each pad on the front side is 20 µm and 10 µm on the rear side. Round copper wires with a diameter of 300 µm are connected to the contact pads on both cell sides by a specified volume of solder (Sn62-Pb36-Ag2).

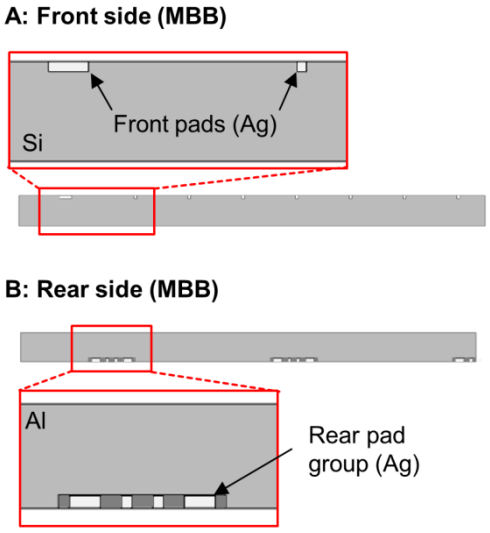

Figure 4: Metallization layout on the front (A) and rear side (B) of the geometry for the MBB model.

2.2 Simulation mesh

The used mesh for the stress simulation consists of tetrahedrons and prisms and its elements are smaller around the solder joint edges to increase the model precision in this area. Figure 5 shows the mesh that is used for the 3BB model. The front side in the area where the end of the busbar is located is displayed.

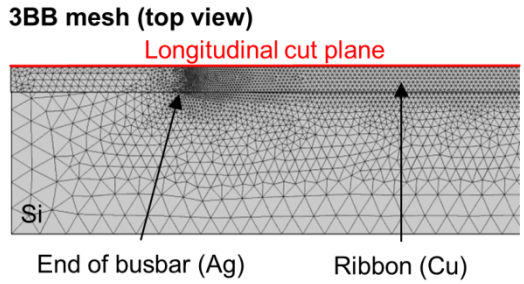

Figure 5: Details of the mesh that is used in the 3BB model. Finer mesh elements near the end of the busbar are shown. Additionally, the red line shows the top edge of the longitudinal cut plane (see figure 1) in the model geometry.

Figure 6 shows the mesh of the MBB model in the area of one pad on the front side.

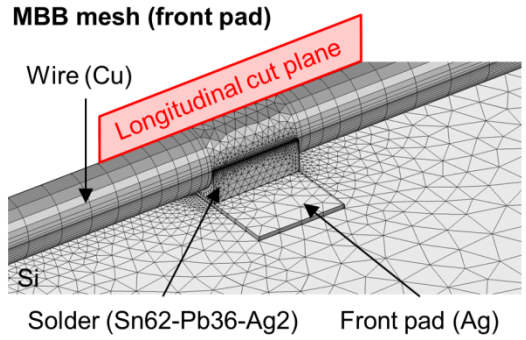

Figure 6: Details of the mesh used in the model for a solar cell with MBB interconnection. The mesh in the area of one small pad on the front side is displayed. Additionally, the red box shows how the longitudinal cut plane (see figure 3) is located in the model geometry.

2.3 Material models

The material data used in the model are measured or respectively taken from literature. A linear elastic material model is used for the silicon, the silver paste and the solder. Additionally, the silicon model includes an anisotropic Young's modulus and a temperature dependent CTE. The bilinear material model for the copper (ribbons and wires) and the aluminum paste includes plastic deformation with hardening when exceeding their yield strength. A FEM model using the material data shown in table I delivers reasonable results, which we previously verified by experimental results [7].

Table I: Material parameters used for the FEM simulation

Material	Young's mod. [GPa]	Yield strength [GPa]	Harden. gradient [GPa]	CTE [$10^{-6}\cdot K^{-1}$]
Bilinear material model				
Al paste [9,10]	6	28.3	0.06[1]	15.9
Copper	70	100	30	17.0 [10]
Linear material model				
Sn62-Pb36-Ag2 [11]	16	-	-	23.9
Ag paste [9,10]	7	-	-	10.0
Silicon [12,13]	Stiffness matrix[2]	-	-	Value table[3]

[1]Assumption of a moderate growth of the stress when increasing the strain level above the yield point
[2]The material model for silicon includes an anisotropic Young's modulus
[3]The Material model for silicon includes temperature dependency of the CTE

2.4 Temperature sweep

The simulation starts at the assumed stress-free state of 179 °C, which is the solidus temperature of the solder, and the whole solder volume is supposed to be solid. Subsequently, the model temperature decreases in steps of 1 K until the target temperature of 20 °C is reached.

3 RESULTS

Silicon is much more prone to defects caused by tensile stress than by compressive stress [14]. Our results indicate that the maximum levels of the third principal stress (compressive stress) in the copper ribbons (53 MPa) and wires (57 MPa) does not exceed their yield strength of 100 MPa. For these reasons we focus on the first principal stress (tensile stress) in the copper interconnector and the silicon caused by their CTE mismatch. Hence the first principal stress in the longitudinal cut plane of both models (see fig. 1 and 3) is shown in the following figures.

3.1 Three busbar solar cell

As shown in figure 7 the tensile stress in the ribbon is induced at the outermost contact on the cell surface – the end of the busbar on the front side and the edge of the first pad on the rear side of the solar cell section. Both interconnectors, on the front and on the rear side, undergo plastic deformation since the maximum tensile stress is about 145 MPa in the front ribbon and 143 MPa in the rear ribbon.

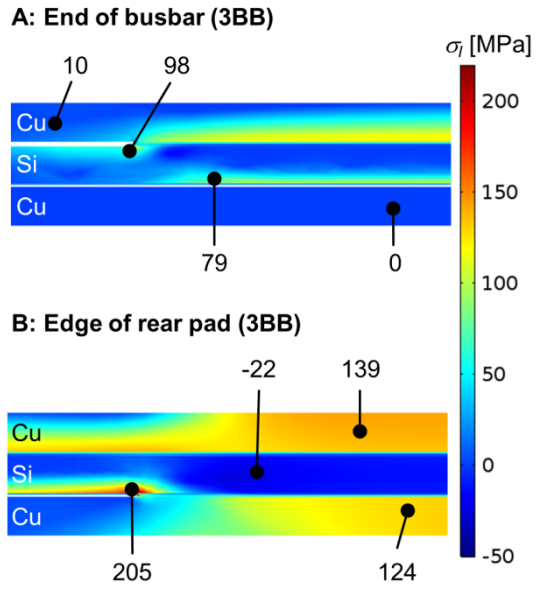

Figure 7: Distribution of the first principle stress in the longitudinal cut plane (see figure 5) of a solar cell with 3BB interconnection. The end of a busbar (A) and the edge of the first rear pad (B) are shown.

In most areas in the silicon there is only small tensile stress. However, we find a local stress peak in the range of 100 MPa near the end of the busbar. In addition, there is a stress peak in the silicon that exceeds 200 MPa adjacent to the first rear pad that can possibly provoke a crack in the silicon.

3.3 Multi Busbar solar cell

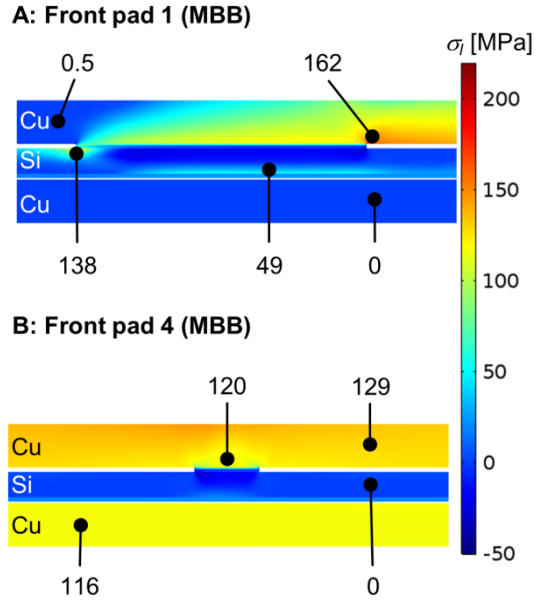

Figure 8: Distribution of the first principle stress in the cut plane (see figure 6) through a solar cell with MBB interconnection. The first pad (A) and the fourth pad (B) of a pad row on the front side are displayed.

Figure 8 and 9 show the distribution of the first principal stress in a MBB solar cell. The tensile stress in the wires is induced at the outermost contact pads on both sides of the cell section. The maximum stress reaches around 160 MPa in the front wire and about 150 MPa in the rear wire. We find nearly homogeneous stress levels of approximately 129 MPa in the front wire and 116 MPa in the rear wire between the contact pads. Additionally, we determine lower stress in the wires adjacent to contact pads on the front (120 MPa) and on the rear side (113 MPa).

The MBB model shows small tensile stress in most parts of the silicon. However, as for the 3BB model, we find local stress levels in the silicon around 140 MPa adjacent to the first front pad and above 200 MPa adjacent to the first rear pad. That may cause a crack in the silicon after the interconnection process.

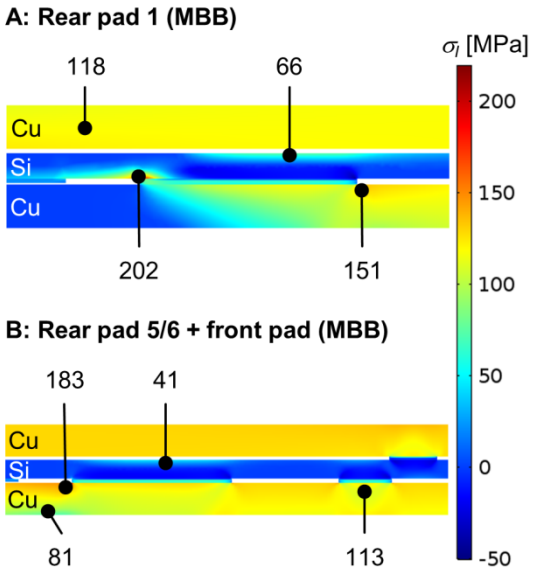

Figure 9: Distribution of the first principle stress in the cut plane (see figure 6) through a solar cell with MBB interconnection. The first pad (A) and two pads of the second pad group (B) on the rear side are displayed.

4 CONCLUSION

This work presents two FEM models to determine the distribution of the thermomechanical stress in solar cells. The models are based on previously published work that deals with the simulation of the single-side soldering of a cell section, including one MBB pad row [7]. In the first model we simulate a solar cell with a common busbar-based interconnection. With the second model the stress in a solar cell interconnected by means of a pad and wire based approach is analyzed. Both models allow the determination of maximum stress areas in a solar cell after the interconnection process.

The model results show a tensile stress in the ribbons up to 145 MPa and in the wires up to 183 MPa, which exceeds their yield strength of 100 MPa and indicates that the copper material undergoes plastic deformation after the soldering process, regardless of the interconnection technology. Adjacent to the contact pads, the stress is slightly lower than in between them. Hence, we expect cold-hardening in the copper material due to the interconnection process that certainly influences the reliability of the solder joints [8].

Due to the interconnection with two identical interconnectors on both sides, the results show only a moderate bending deformation of the cell section of about 0.4 mm with 3BB and respectively 2.2 mm with

MBB interconnection. In both cases that deformation is caused by the non-symmetrical metallization layout and we expect these bending levels to be noncritical for the lamination process.

In most parts of the silicon the tensile stress is comparatively low. However, there are stress maxima in the silicon near the outermost contacts with the copper interconnectors. On the front side we determine a maximum stress of nearly 100 MPa for 3BB interconnection and about 140 MPa for cells with MBB approach. With regards to fracture stresses in silicon published by Kaule et al. [14] these stress levels are not expected to be critical. On the rear side we determine significantly larger tensile stress due to the interconnection. We find maximum stresses in the range of 200 MPa in the 3BB model as well as in the MBB model. These critical areas are prone to defects caused by the interconnection of 3BB and MBB solar cells. Potential defects after the solder process or during its lifetime result in an increase of the series resistance of a solar module and therefore reduce the module efficiency. In case of solder joint defects, cell fracture or broken interconnectors the series resistance of solar modules with MBB concept increases less than of 3BB modules due to the large number of redundant interconnecting wires [4]. Since we find no significant difference of the mechanical stress maxima we expect the solar modules with MBB interconnection technology to show advantages in terms of long-term stability.

In further work it is possible to use both models to determine the influence of the material parameters on the thermomechanical stress by parameter studies.

5 REFERENCES

[1] J. Walter, M. Tranitz, M. Volk, C. Ebert, and U. Eitner, "Multi-wire Interconnection of Busbar-free Solar Cells," Energy Procedia 55, 2014, pp. 380-388.

[2] S. Braun, G. Micard, and G. Hahn, "Solar cell improvement by using a multi busbar design as front electrode," Energy Procedia 27, 2012, pp. 227-233.

[3] S. Braun, G. Hahn, and R. Nissler, "Multi-Busbar solar cells and modules: high efficiencies and low silver consumption," Energy Procedia 38, 2013, pp. 334-339.

[4] A. F. Dethlefsen, M. Volk, K. Ramspeck, and C. Buchner, “Reliability Testing of Multi-Busbar Modules,” EUPVSEC, Amsterdam, Nederlands, 2014.

[5] S. Schindler, J. Schneider, C. Poenisch, R. Nissler, and D. Habermann, “Soldering process and material characterization of miniaturized contact structures of a newly developed multi busbar cell metallization concept,” EUPVSEC, Paris, France, 2013.

[6] T. Söderström, P. Papet, and J. Ufheil. "Smart wire connection technology," EUPVSEC, Paris, France, 2013.

[7] L. C. Rendler, J. Walter, T. Geipel, M. Volk, C. Ebert, and U. Eitner, “Modelling and Verification of Mechanical Stress Induced by Soldering of Wires for Multi Busbar Interconnection”, EUPVSEC, Hamburg, Germany, 2015.

[8] R. Meier, M. Pander, R. Klengel, S. Dietrich, S. Klengel, M. Ebert, and J. Bagdahn, "Reduction of soldering induced stresses in solar cells by microstructural optimization of copper-ribbons," in SPIE Solar Energy+ Technology, 2011.

[9] C. Kohn, T. Faber, R. Kübler, J. Beinert, G. Kleer, F. Clement, D. Erath, I. Reis, F. Martin, and A. Müller, "Analyses of warpage effects induced by passivation and electrode coatings in silicon solar cells," EUPVSEC,Milan, Italy, 2007.

[10] S. Wiese, F. Kraemer, E. Peter, and J. Seib, "Mechanical problems of novel back contact solar modules," EuroSimE, Cascais, Portugal, 2012.

[11] Q. Zhang, "Isothermal Mechanical and Thermomechanical Durability Characterization of Selected Pb-free Solders," Doctor of Philosophy, Department of Mechanical Engineering, University of Maryland, 2004.

[12] U. Eitner, S. Kajari-Schroeder, M. Koentges, and H. Altenbach, "Thermal stress and strain of solar cells in photovoltaic modules," in Shell-like Structures: Non-classical Theories and Applications. vol. 15, Springer, 2011, pp. 453-468.

[13] K. G. Lyon, G. L. Salinger, C. A. Swenson, and G. K. White, "Linear thermal expansion measurements on silicon from 6 to 340 K," Journal of Applied Physics, vol. 48, 1977, pp. 865-868.

[14] F. Kaule, W. Wang, and S. Schoenfelder, “Modeling and testing the mechanical strength of solar cells,” Solar Energy Materials and Solar Cells, vol. 120, 2014, pp. 441–447.